Maritime Technology and Research

https://so04.tci-thaijo.org/index.php/MTR

Research Article

Response control of TLP with single TMD under wind, wave, and current

Suja T. P.[1] and Srinivasan Chandrasekaran[2,3,*]

[1]*Department of Civil Engineering, Manipal Institute of Technology, Manipal Academy of Higher Education, India*
[2]*Department of Ocean Engineering, Indian Institute of Technology Madras, India*
[3]*International Maritime Studies, Kasetsart University, Sriracha Campus, Chonburi 20230, Thailand*

[*]*Corresponding author's e-mail address: drsekaran@iitm.ac.in; srinivasan.c@ku.th*

Article information

Received: May 14, 2024
Revision: July 9, 2024
Accepted: July 23, 2024

Keywords
Tension leg platform (TLP);
Single-tuned mass damper (TMD);
Surge control;
Power Spectral Density (PSD);
Phase plots;
Recentering

Abstract

Offshore Tension Leg Platforms (TLP) are hybrid structures that encounter large offsets under rough sea states. They impose large displacements, resulting in operational challenges under extreme sea states. The key to safe topside operation is to minimize responses in flexible modes using appropriate control mechanisms. The present study evaluates the response control of TLP with tuned mass damper under different sea state environments. The damper is positioned such that the mass center of the primary and secondary system is concurrent. It is enabled only with surge motion, which controls the platform surge motion by tuning their frequency ratios. Response control in surge motion is assessed for different mass ratios of the damper. Results show that the RMS value of surge response is effectively reduced for a mass ratio of 0.3, while other mass ratios do not show effective control; the maximum reduction in the surge amplitude is about 26 %. The response reduction is essentially due to the phase shift between the nature of the responses with and without tuned mass damper. In addition, the damper helps improve the recentering capabilities observed from the phase plots.

1. Introduction

Deep-water oil exploration in rough sea states is challenging due to the severe loads encountered (Chandrasekaran & Jain, 2016; Chandrasekaran & Koshti, 2013; Chandrasekaran & Nagavinothini, 2020; Chou et al., 1980; Sreenivasan et al., 2021). Environmental loads, particular wind, pose serious complexities for offshore structures (Hongbo et al., 2022). Geometric forms of compliant offshore platforms inhibit a high degree of flexibility (also called compliancy) in the plane of horizontal motion while maintaining rigidity in the vertical plane (Yoneya & Yoshida, 1981; Srinivasan & Purushotham, 2024). Offshore Tension Leg Platforms (TLPs) are hybrid structures, designed to operate in deepwater environments. TLPs are designed to achieve large periods in surge, sway, and yaw motion, while heave, roll, and pitch are fixed at very low periods. Such a hybrid combination makes TLPs well-suitable for deep-water drilling, but with a compromise on large displacements in the horizontal plane (Wang & Kim, 2001). Therefore, this imposes a serious

limitation on the payload of the TLP deck. While coupling between surge and heave, often referred to as offset and set down, helps compensate for this limitation to some extent, large surge motion remains a challenge. Researchers addressed this concern by optimizing the shape of TLP; three-legged TLPs showed fewer responses (Abou-Rayan & El-Gamal, 2013; Chandrasekaran & Jain, 2002; 2001).

TLPs are designed for excessive buoyancy compared to their weight (Chandrasekaran et al., 2013; 2007b; 2007d; 2007c; 2004); this buoyancy is compensated for by high initial pre-tension in tethers, which position-restrain TLPs to the sea bed. While commissioning, initial stability of the TLP is achieved by the force balance between its weight, buoyancy, and initial pre-tension in the tethers (Chandrasekaran et al., 2006a, 2006b). However, under wave action, there exists a continuous variation in tether tension to compensate for the surge-heave coupling effects (Chandrasekaran et al., 2007a). In case of impact caused by multiple ship collision, excessive loads imposed on the hull govern the stability and survival of the offshore vessels. It is interesting to note that, even in the situation of plug-out failure of tethers, TLPs do not capsize, as they are positively buoyant; thus, possessing high hydrodynamic stability (Chandrasekaran, 2015). Studies showed a satisfactory response of TLPs under seismic excitations as well (Chandrasekaran & Gaurav, 2008). Under extreme wave conditions, the springing and ringing responses are more instead of high, creating malfunctioning of the platform, which is a challenge to be counted (Chandrasekaran & Jamshed, 2017; Chandrasekaran & Nassery, 2017; Srinivasan et al., 2011).

TLPs have two distinct bands of natural frequencies in stiff and flexible degrees of freedom, which are intentionally designed to isolate them from the frequency bandwidth of oceanic waves effectively. Due to the inherent compliancy of TLPs in the plane of horizontal motions, they exhibit large offsets under extreme sea states which can result in several operational challenges. The excessive dynamic movements of TLPs can not only hamper topside operations, such as drilling, production, and other routine activities, but also affect risers and subsea equipment, which can lead to the fatigue of risers and production mains, or even their possible disconnection from the platform. Additionally, the large motion can also cause discomfort and motion sickness for personnel on board, thereby impacting their overall efficiency. The key to safe topside operations is to minimize the response in flexible modes. To address these challenges, various engineering and operational strategies have been investigated to enhance platform performance and safety under extreme sea conditions. One of the strategies, i.e., the use of appropriate response control mechanisms, is commonly reported in the literature (Kandasamy et al., 2016).

Over the past decade, several researchers attempted to control response in different degrees of freedom and stabilize TLP motion for its satisfactory performance (Tabeshpour & Malayjerdi, 2021). The main classifications of vibration control are active and passive control strategies. They are broadly grouped as Tuned Mass Dampers (TMD), Multiple Tuned Mass Dampers (MTLD), Tuned Liquid Dampers (TLD), and Tuned Liquid Column Dampers (TLCD). The latter is common in ship motion control, and the former is preferred for compliant offshore platforms such as TLPs. Tuned mass dampers offer better passive control strategies for closely spaced frequency modes (Taflanidis et al., 2009). This is attributed to the fact that TLPs possess a strong coupling of surge and heave motion. As TLPs are positive-buoyant and possesses high reserve capacity in heave motion, tuned mass dampers suspended from decks can offer resistance to surge motion without any heave compensation (Chandrasekaran et al., 2013; 2015). Chatterjee and Chakraborty (2014) conducted a numerical study to mitigate wave-induced vibrations in TLP structures using TLCD and

TLCBD; the comparative study showed that TLCBD outperforms TLCD in wave vibration reduction.

Based on the literature, it can be seen that this topic needs further investigation, although some attempts have been made in the past to address the challenges. The primary aim of this research is to find the effectiveness of a single-tuned Tuned Mass Damper (TMD) in mitigating surge responses. The study also focuses on modeling a TMD using commercially available packages, which can aid in further developing this proof of concept. In the present study, an ISSC TLP is numerically assessed under different sea state environments, and its responses in the presence of a single-tuned Mass Damper (TMD) are compared. In this study, concurrent wave-wind-current with zero-degree wave heading angle is considered, and the responses in the active degrees of freedom (i.e., surge, heave, and pitch) are revealed. The wave directionality effects with all six degrees of freedom active will be investigated as a subsequent part of this study; hence, the same is not covered in the present work.

Table 1 ISSC TLP geometric details (Eatock Taylor & Jefferys, 1986; Xu et al., 2022).

Description	**Quantity**
Diameter of columns (m)	16.88
spacing between columns (m)	86.25
Pontoon dimension (m)	7.50×10.50
Water depth (m)	450.0
Draft at MWL (m)	35.0
Platform DWT (tons)	40,500
Centre of gravity above keel (m)	38.0
Mass moment of inertia along roll (I_{XX}) (kg-m^2)	82.37×10^9
Mass moment of inertia along pitch (I_{YY}) (kg-m^2)	82.37×10^9
Mass moment of inertia along yaw (I_{ZZ}) (kg-m^2)	98.07×10^9
Length of tendons (m)	415.0
Combined vertical stiffness of tendons (kN/m)	813×10^3

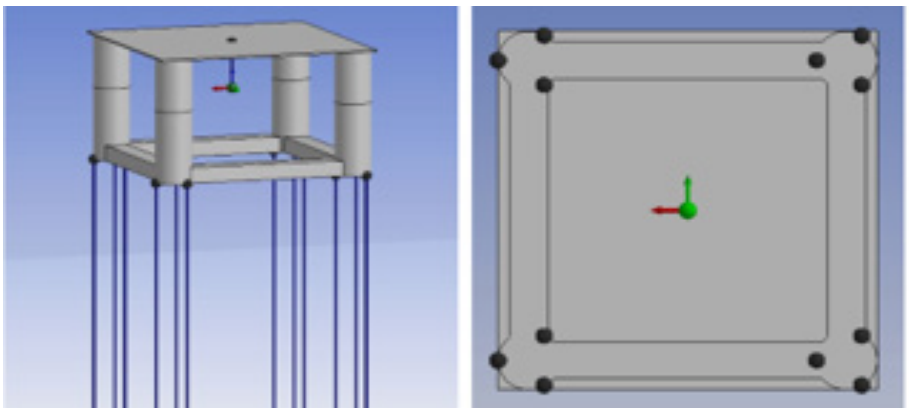

(a) 3D view (b) Bottom plan view

Figure 1 Schematic diagram of ISSC TLP.

2. ISSC TLP specifications

The geometric details of the ISSC TLP, which are taken into consideration for this case study, are tabulated in **Table 1** (Eatock Taylor & Jefferys, 1986; Xu et al., 2022). The ISSC TLP geometry consists of four buoyant columns, each with diameter 16.88 m and spaced at 86.25 m. The columns are interconnected by a floating box of pontoon of a width of 7.50 m and a height of 10.50 m. The TLP hull is attached to the three tensioned tendons per leg at the keel location. **Figure 1** depicts a schematic diagram of the TLP geometry. The TLP has a draft of 35m below the mean water level (MWL). The TLP is anchored to the seabed at 450 m below the MWL. The center of gravity of the platform lies 38 m above the keel.

2.1 Environmental conditions

In this section, the specifications for the sea state environments considered in this investigation are outlined. To confirm the proof of concept under different environmental conditions, the ISSC TLP is subjected to three different sea state environments i.e., moderate sea state, high sea state, and very high sea state. **Table 2** summarizes the wind and wave parameters used in the analysis. The statistical parameters, namely significant wave height (Hs), zero crossing period (Tz), and wind velocity, are used to describe each sea state. A modified Pierson-Moskowitz (P-M) spectrum with a zero-degree wave heading angle is chosen for the present study. The typical P-M spectrum curve for the different sea states and the Gulf of Mexico (GoM) wind-induced 3-point current profile considered in the present study is also shown in **Figure 2**. The current profile is defined by a surface current velocity of 0.5 m/s, uniform through 60 m depth below sea water level (SWL) which is reduced linearly to a minimal current velocity of 0.1 m/s at a depth of 90 m and remains constant up to 200 m below SWL. The concurrent wave-wind-current parameters considered in the case study are based on the study carried out by (Nagavinothini & Chandrasekaran, 2019).

Table 2 Sea states considered for the case study (Nagavinothini & Chandrasekaran, 2019).

Sea state	Moderate	High	Very high
Wave approach angle	0°	0°	0°
Wave height, H_s (m)	6.5	10	15
Wave period, T_Z (sec)	8.15	10	15
Wind speed (m/s)	15	35	45
Wind directional offset with respect to wave	0°	0°	0°

3. Numerical modeling and analysis

This section covers the numerical modeling and analysis of ISSC TLP with and without the tuned mass damper. The detailed modeling of ISSC TLP in Ansys Workbench is presented herein. The section has two subsections: the first sub-section 3.1 presents verification of the ISSC TLP numerical model with the reference study, whereas the second sub-section 3.2 gives the mathematical formulation for a single TMD and its modeling aspects in ANSYS Workbench.

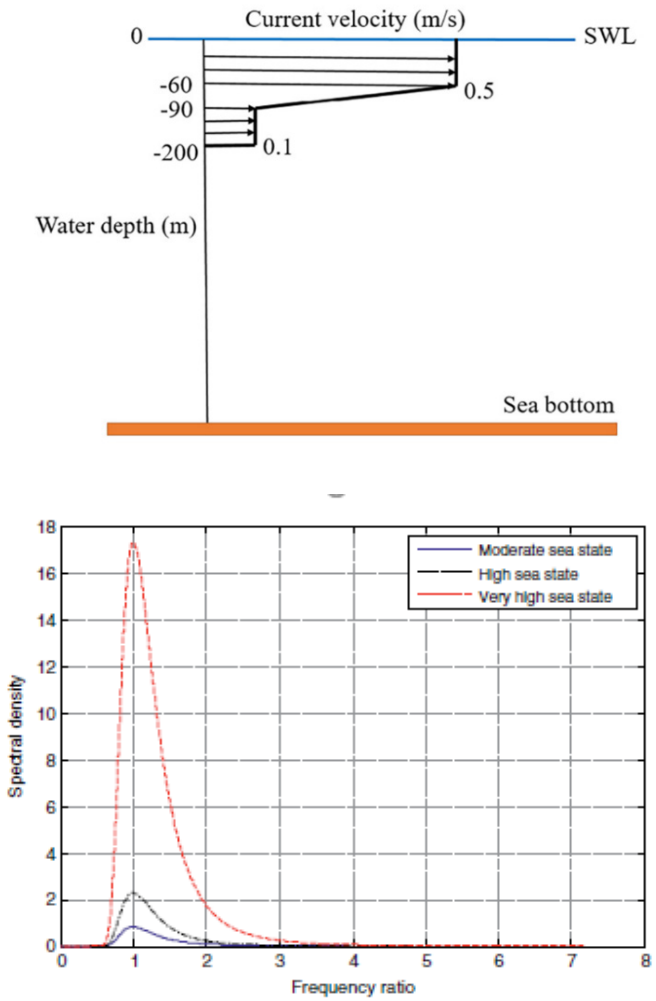

Figure 2 PM spectrum and current profile (Nagavinothini & Chandrasekaran, 2019).

The ISSC TLP is numerically modeled in the hydrodynamic diffraction and hydrodynamic response analysis system of ANSYS Workbench 2022 R1. ISSC TLP geometry, developed in ANSYS Space Claim, is imported into the hydrodynamic analysis module of ANSYS. The specifications of the ISSC TLP, such as geometric, mass, and inertia properties mentioned in **Table 1**, are assigned to the model. The hull of the TLP is modeled as a diffraction convolution element. The geometry is then meshed into 32,659 nodes and 32,693 elements with maximum element size restricted to 2 m to ensure convergence. The meshed geometry of ISSC TLP is depicted in **Figure 3**. Linear cable elements are used to model the tendons, connecting the keel points on the lower hull to a fixed point on the sea bed at 450 m below MWL. A vertical stiffness of 67,750 kN/m and an unstretched length of 415 m are assigned to each tendon. The numerical model of ISSC TLP is depicted in **Figure 5**. The wave, wind, and current parameters are as stated in section 2.1 Environmental conditions are set in the ANSYS Hydrodynamic Response Analysis system. The input wave load is given by the P-M spectrum with a wave heading angle of zero degrees, which is mathematically shown below:

$$s(\omega) = 5\pi^4 \frac{H_s^2}{T_p^4} \frac{1}{\omega^5} \exp\left[-\frac{20\pi^4}{T_p^4} \frac{1}{\omega^4}\right] \quad (1)$$

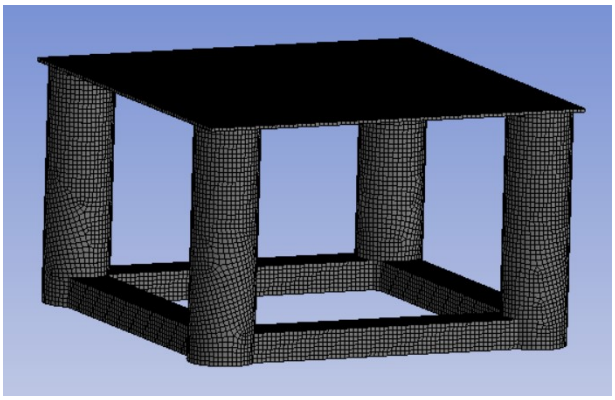

Figure 3 Meshed geometry of ISSC TLP.

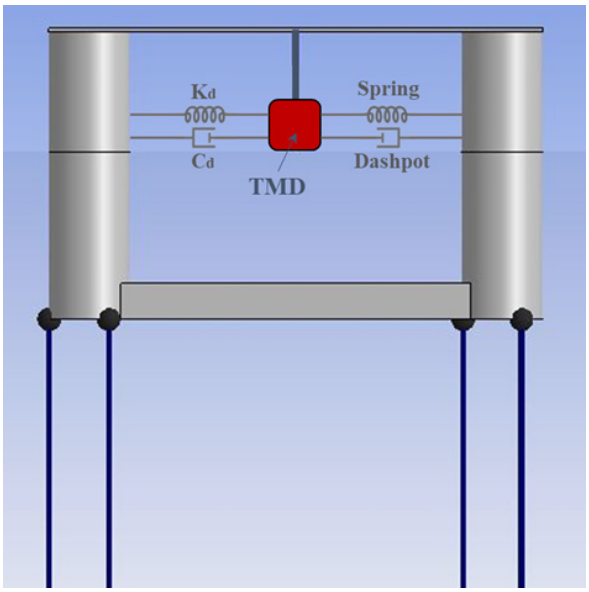

Figure 4 Mathematical model of a single TMD attached to ISSC TLP.

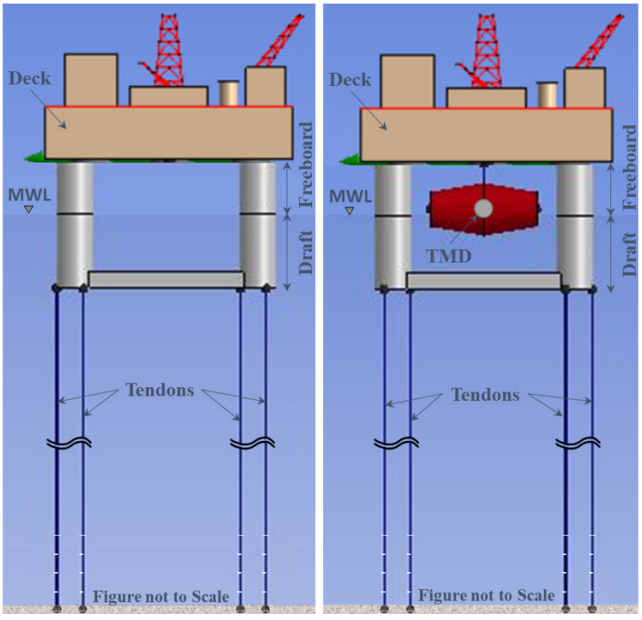

Figure 5 TLP model without and with Tuned Mass Damper (TMD).

The program computes the wave load based on the input wave height and wave period. The wind load is assigned using a program-controlled API wind spectrum with a directional offset of zero degrees concerning the wave. A 3-point current profile is set in the current definition data. The program uses this current profile varying with depth to compute the current load. The current directional offset is set to zero degrees concerning the wave. The wave-wind-current is considered concurrent in this study. Time Domain hydrodynamic response analysis is executed for 1,500 sec with a time step of 0.1 sec. The analysis is carried out for a set of load cases: (i) Wave Alone, (ii) combined Wave and Wind, and (iii) combined Wave, Wind, and Current, each for three different environments, namely, moderate sea states, high sea states, and very high sea states. Initially, the response of the ISSC TLP is assessed for all the nine load cases (i.e., SS-1 to SS-9).

Table 3 Natural frequencies of ISSC TLP.

	Natural Frequencies (rad/s)					
	Surge	**Sway**	**Heave**	**Roll**	**Pitch**	**Yaw**
Present study	0.0644	0.0644	3.116	3.254	3.254	0.0783
Reference study (Xu et al., 2022)	0.0612	0.0612	3.488	3.401	3.401	0.0764

Table 4 Different sea states and combinations.

No	**Description**	**Load combination**
1	SS1	Moderate wave only
2	SS2	Moderate wave and wind
3	SSS3	Moderate wave, wind, and current
4	SS4	High wave only
5	SS5	High wave and wind
6	SS6	High wave, wind, and current
7	SS7	Very high wave only
		Very high wave and wind
		Very high wave, wind, and current

3.1 Validation

To validate the numerical model, the natural frequencies of ISSC TLP without a single TMD, obtained from the hydrodynamic response analysis, are compared with the reference study carried out by Xu et al., 2022. The results are tabulated in **Table 3**. **Table 4** shows the load combinations considered for the study. The observed variation in the natural frequencies can be attributed to alterations in both the configurations and properties of the tendons, as compared to the reference study. The referred literature considered two tendons per leg with different values of tendon stiffness. However, the difference in the results is below 5 %, except for the heave natural frequency. The difference in the heave case is attributed to the use of a lower value of tendon stiffness in this investigation, which is based on the study conducted by Eatock Taylo & Jefferys (1986).

3.2 Modeling of Single Tuned Mass Damper (TMD)

The important parameters to be considered for a single-tuned mass damper are (i) the mass ratio (μ), which is the ratio of the mass of the damper to that of the primary structure, and (ii) the frequency ratio (f) which is the ratio of the frequency of vibration of the damper to the frequency of vibration of the primary structure. The mass and frequency ratios are given by Chandrasekaran et al., 2013;

$$\mu = \frac{m_d}{M} \tag{2}$$

$$f = \frac{1}{1+\mu} \tag{3}$$

where m_d is the mass of the damper; and M is the mass of the primary structure. The natural frequencies of the structure and that of the damper are kept closer (i.e., $\omega \approx \omega_d$) to ensure the maximum dissipation of energy by the damper. Here, ω is the natural frequency of the primary structure in the desired degree of freedom in which the responses are to be minimized; and ω_d is the natural frequency of the damper. For the given mass ratio, the stiffness of the single TMD can be obtained using the following expression:

$$K_d = \mu \cdot K \tag{4}$$

where K_d is the stiffness of the damper; and K is the stiffness of the primary structure in the desired degree of freedom.

For a single TMD, the optimum damping ratio ($\xi_{d,opt}$) and damping coefficient (c_d) (Ayorinde & Warburton, 1980) are expressed as follows:

$$\xi_{d,opt} = \sqrt{\frac{\mu\,(1+0.75\mu)}{4(1+\mu)(1+0.5\mu)}} \tag{5}$$

$$c_d = 2m_d \cdot \xi_{d,opt} \cdot \omega_d \tag{6}$$

where, the mass of the damper, $m_d = \mu \cdot M$;

The inertial force induced in the TMD acts in the opposite direction to that of the motion of the primary structure which dissipates the energy in the primary structure. In ANSYS Workbench, a single TMD is modeled as a non-diffracting secondary structure, consisting of a spring-mass-dashpot, suspended from the deck of the primary TLP structure as shown in **Figure 4**. This secondary structure is assigned to a mass point that has the mass properties of the TMD, which vary for the different tuned mass ratios. The secondary structure is placed in such a manner that its mass center coincides with the mass center of the primary TLP structure. An inextensible linear cable suspends the TMD from the deck of TLP, as shown in **Figure 4**. The uni-directional fender elements are used to model the spring and dashpot system for the secondary structure.

For the different tuned mass ratios, the optimum stiffness and damping are assigned to TMD using fender elements. The fender elements are oriented in such a manner that the restoring and damping forces are transmitted to the primary TLP structure. All the degrees of freedom of the TLP, except surge, are restrained to ensure unidirectional movement of the TMD. The TLP is proposed to control only the platform surge motion in the present study. The numerical model of ISSC TLP is depicted in **Figures 4** and **5**. The time domain dynamic analysis is performed for the ISSC TLP model with TMD under wave wave-alone environment for a set of mass ratios ranging from 0 to 1.0 in a multiple of 0.1 to find the effective mass ratio. A total of 11 cases are considered to find the effectiveness of the TMD, with the first being the case of TLP without TMD (i.e., $\mu = 0$) which is used to compare the percentage reduction in surge response. For every mass ratio, mass, stiffness, and damping properties of the TMD are computed using Eqs. (2), (4), and (6), respectively. These values are assigned to the secondary structure and the fenders. Time domain hydrodynamic response analysis with a time step of 0.1 sec is carried out for all 11 cases, and the statistical responses are noted. An effective response control is achieved for a mass ratio (0.2 to 0.3) resulting in effective response control; higher mass ratios, apart from being not feasible, were also found to be ineffective (Chandrasekaran & Suja, 2023). Based on the results, a mass ratio of 0.3 is selected for further investigation of the ISSC TLP model with TMD under the load cases: (i) Wave Alone, (ii) combined Wave and Wind, and (iii) combined Wave, Wind, and Current, each for three different sea states, namely, moderate, high, and very high. In total, nine load cases (i.e., SS-1 to SS-9) are considered for ISSC TLP with TMD, and the responses are compared with those of the ISSC TLP model. The responses associated with the surge, such as heave and pitch, are obtained, whereas the other degrees of freedom, such as sway, roll, and yaw, are deactivated, to see the effectiveness of the single TMD in controlling the surge responses. The results and comparisons are outlined in section 4.

4. Results and discussion

This section presents the results obtained from the time domain analysis for ISSC TLP without and with TMD having a mass ratio of $\mu = 0.3$ for different sea state conditions (i.e., SS-1 to SS-9). Detailed discussions on the results are also presented. Subsection 4.1 covers sea states with wave alone environment (i.e., SS-1, SS-4, and SS-7); subsection 4.2 covers sea states with combined wave and wind (i.e., SS-2, SS-5, and SS-8); whereas subsection 4.3 includes sea states with a combined wave, wind, and current (i.e., SS-3, SS-6, and SS-9). Each subsection presents response time histories and power spectral densities (PSDs) of the responses in all active degrees of freedom (i.e., surge, heave, and pitch) for the above-stated load cases. In addition, the phase plots in surge degree-of-freedom are also presented in each subsection. In the end, the periods and damping, as well as the response statistics, in all active degrees of freedom for different environmental conditions, are presented in tabular form.

4.1 Wave alone

Figures 6a - 6c shows the surge responses for the ISSC TLP without and with TMD having a mass ratio of $\mu = 0.3$ under different sea state environments with wave-alone conditions. It can be observed from the surge response time histories that there is a substantial reduction in surge motion with the use of the TMD for moderate sea state. The surge response of the TMD, highlighted with an orange dotted line in **Figure 6**, deliberately overlapped that of the TLP to show the effectiveness of

the TMD in mitigating the surge responses. It has been noticed that the surge responses exhibit a reduction of about 25 percent for moderate sea states; however, for high and very high sea states, the response control does not happen. The root mean square values for the surge responses show a reduction of about 22 percent for moderate; about 2 percent for high sea states; and about 6 percent for very high sea states. The reduction in the surge motion is essentially due to the phase shift between the nature of the responses with and without TMD. It can be observed that the heave and pitch responses are not influenced by the presence of the TMD. The mean, rms, and maximum responses in the heave and pitch remain almost unchanged, which is the added advantage of a system with TMD.

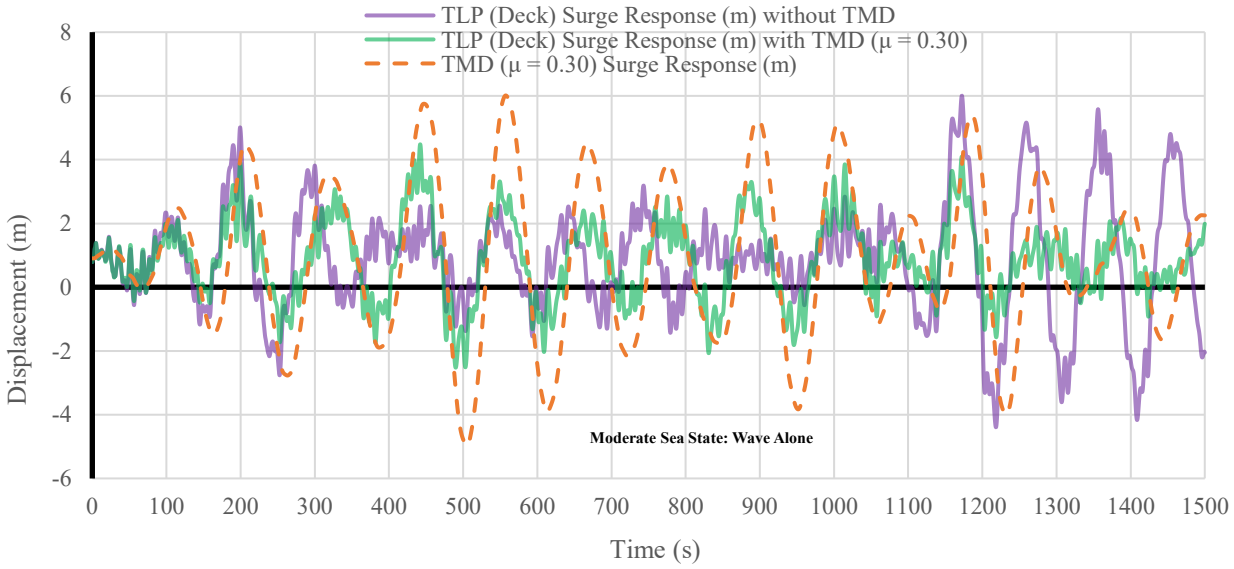

(a)

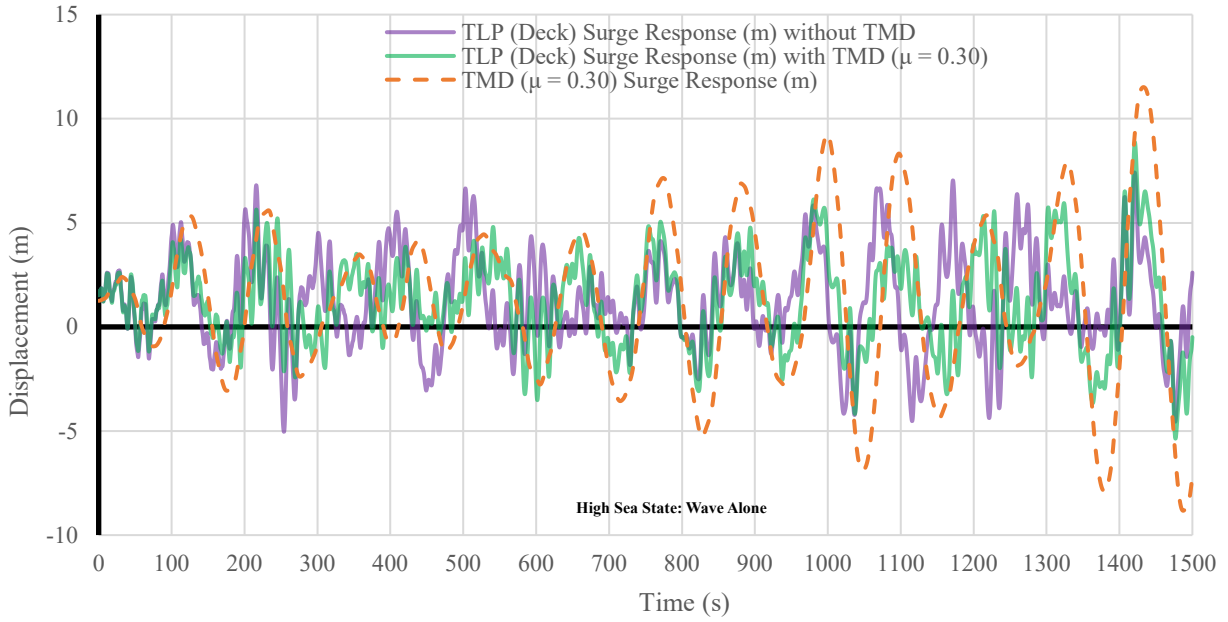

(b)

Figure 6 Wave alone case, (a) surge responses under moderate sea state, (b) surge responses under high sea state, (c) surge responses under very high sea state.

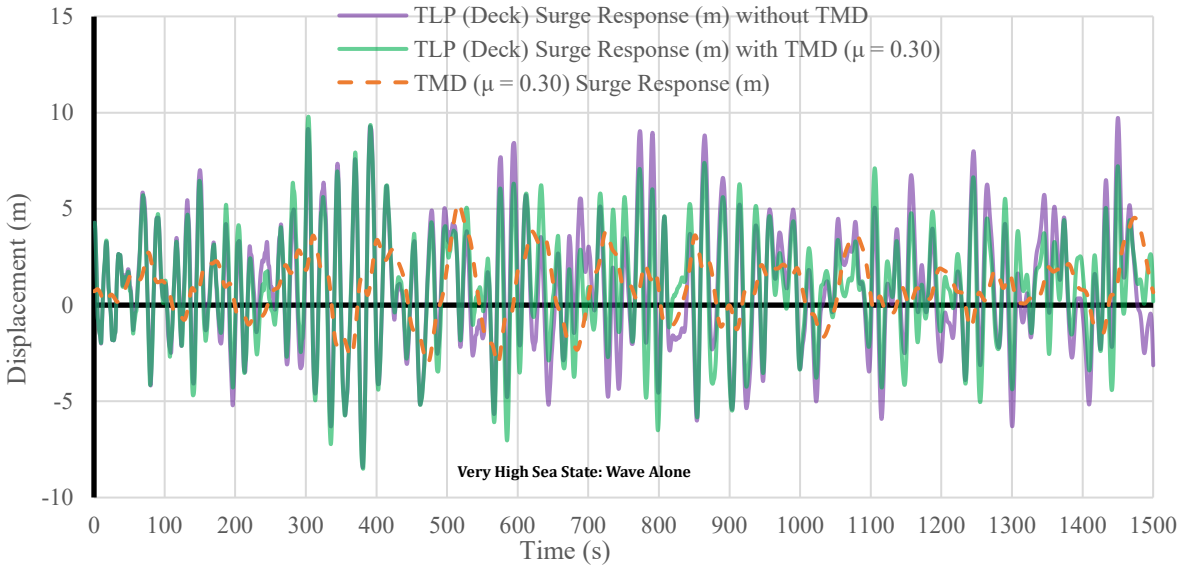

(c)

Figure 6 (continued) Wave alone case, (a) surge responses under moderate sea state, (b) surge responses under high sea state, (c) surge responses under very high sea state.

The power spectral densities in the surge are depicted in **Figures 7a - 7c**. The PSD plots show a significant reduction in the energy content in the surge degree of freedom, about 50 percent for moderate and very high sea states. However, it has been observed that the TMD is ineffective under a high sea state. The other degrees of freedom, heave and pitch, do not show much variation in PSD plots. The shifts in the natural frequencies with and without TMD are shown with dotted lines in the PSD plots. It is seen that shifts in the natural frequencies due to the presence of the TMD are marginal. The peak in the surge PSD closely corresponds to the surge natural frequency for both models, which needs to be taken into consideration for the detailed design by altering the tendon stiffness. **Figures 8a - 8c** show the phase plots for the surge motion under different sea state environments with wave-alone conditions. The phase plots confirm the recentering ability of the platform, which is one of the desirable behaviors of TLP. The study also confirms that the recentering capabilities of the platform are not affected by the additional damping induced by TMD.

4.2 Combined wave and wind

The surge responses for the ISSC TLP without and with TMD having a mass ratio of $\mu = 0.3$ under combined wave and wind conditions of different sea state environments are depicted in **Tables 5** and **6**, respectively. The responses under combined wave and wind case follow similar trends as seen for the wave alone case. The surge response time history shows a significant reduction in the surge motion for a moderate sea state in the presence of the TMD. It has been found that the response reduction in the surge is about 25 percent for moderate sea states, the same as for the case of wave alone. However, the response control for high and very high sea states does not happen, which can be further investigated using Multiple Tuned Mass Dampers (MTMD). The rms values for the surge responses show a reduction of about 22 percent for moderate; about 1.65 percent for high sea states; and close to 6 percent for very high sea states. The influence of the TMD on heave and pitch responses is absent. Here also, the mean, rms, and maximum responses in the heave and pitch are almost unchanged. Based on the results, it can be observed that the effects of wind load are minimal for the

study under consideration. The PSD plots show a significant reduction in the energy content in the surge degree of freedom, about 50 percent for moderate and very high sea states. However, the TMD is seen to be ineffective under high-sea states. The statistical comparison of the responses for ISSC TLP without and with TMD under different sea states is presented in **Tables 5** and **6**. Interestingly, it is to be noted that the response histories do not register any shift in the mean position of the platform, even in the presence of the TMD, confirming the fact that the recentering capabilities of the platform are not disturbed under external damper. The other degrees of freedom, heave and pitch, do not show much variation in PSD plots. It is seen that shifts in the natural frequencies, due to the presence of the TMD, are marginal (**Tables 7** and **8**).

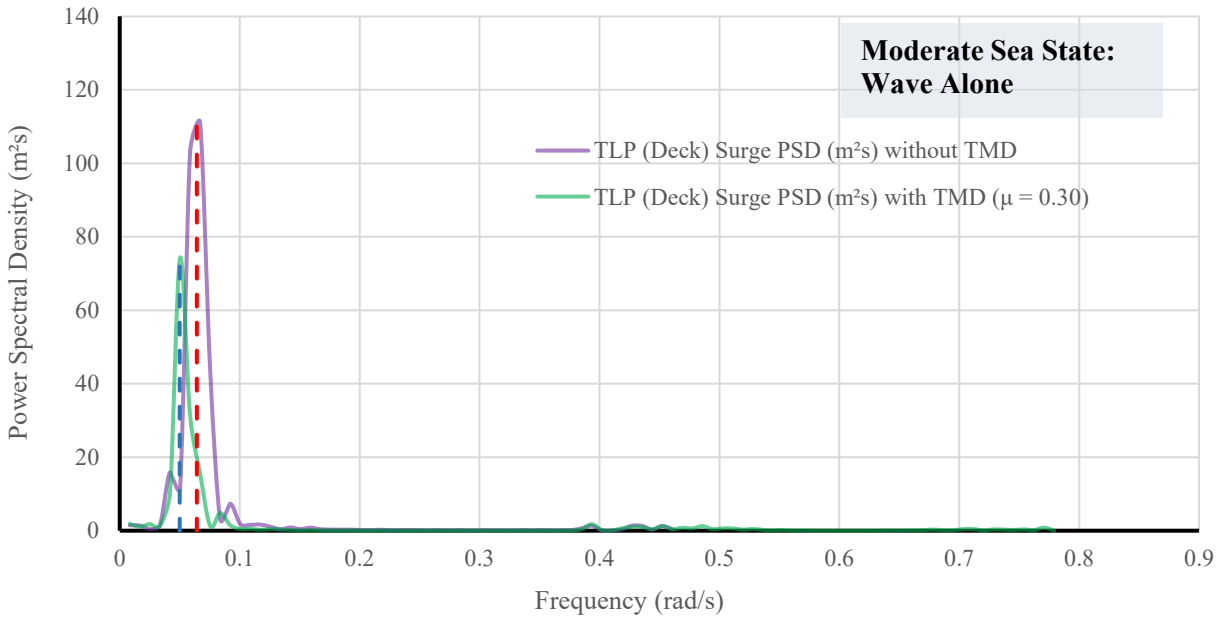

(a)

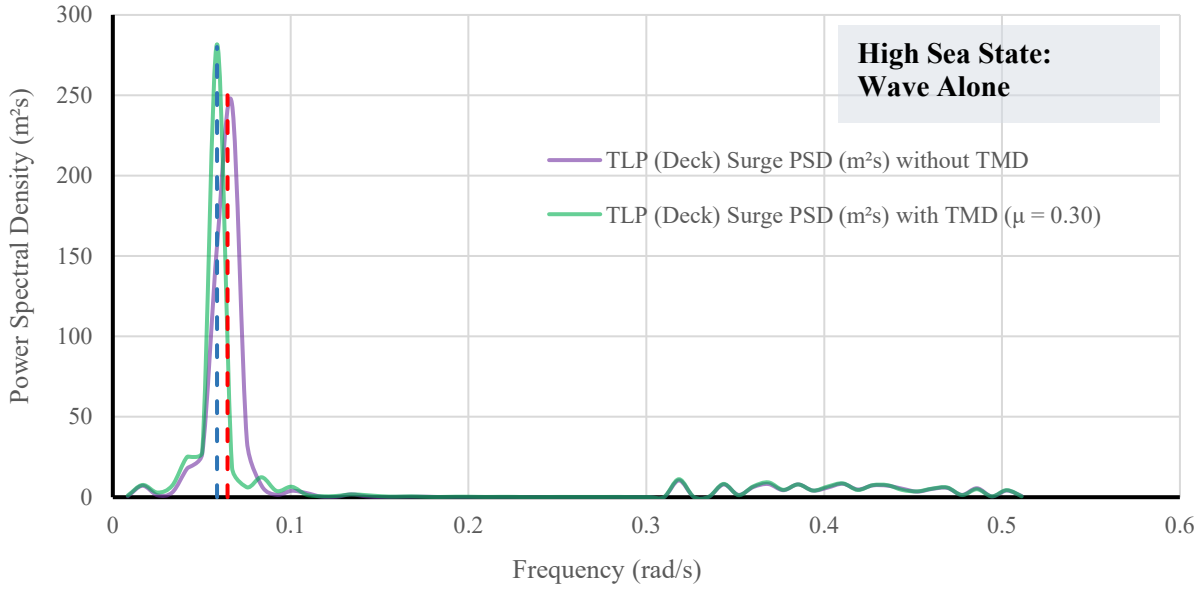

(b)

Figure 7 Wave alone case, (a) surge PSD under moderate sea state, (b) surge PSD under high sea state, (c) surge PSD under very high sea state.

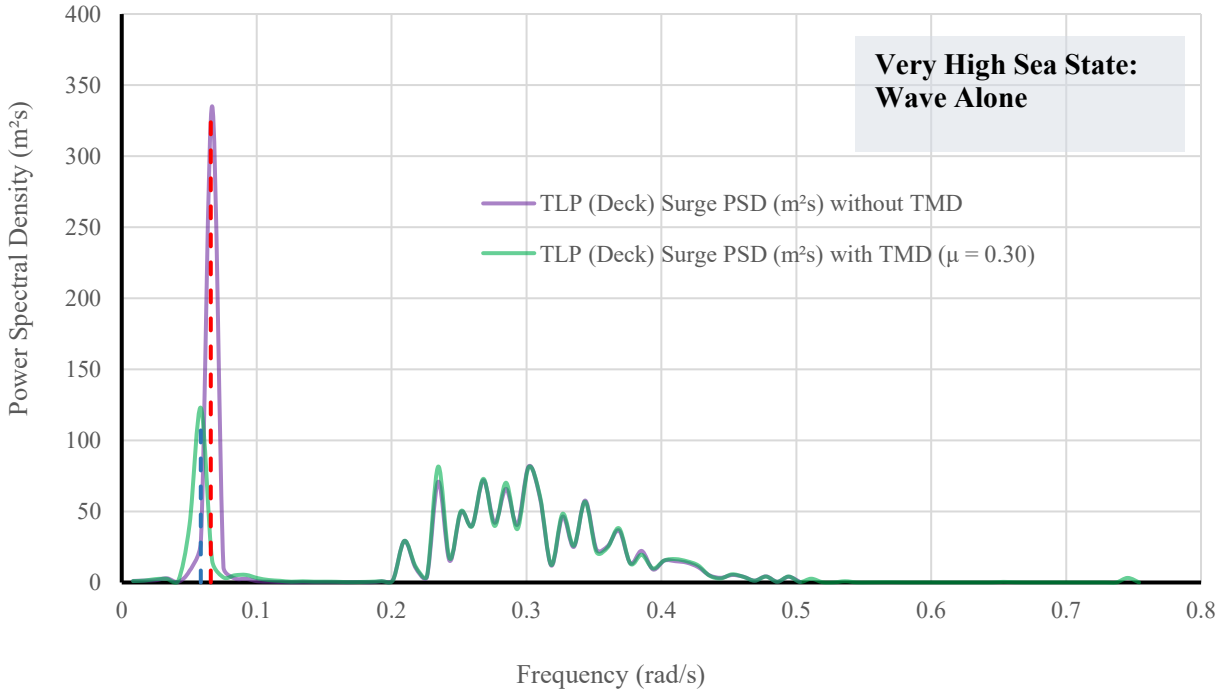

(c)

Figure 7 (continued) Wave alone case, (a) surge PSD under moderate sea state, (b) surge PSD under high sea state, (c) surge PSD under very high sea state.

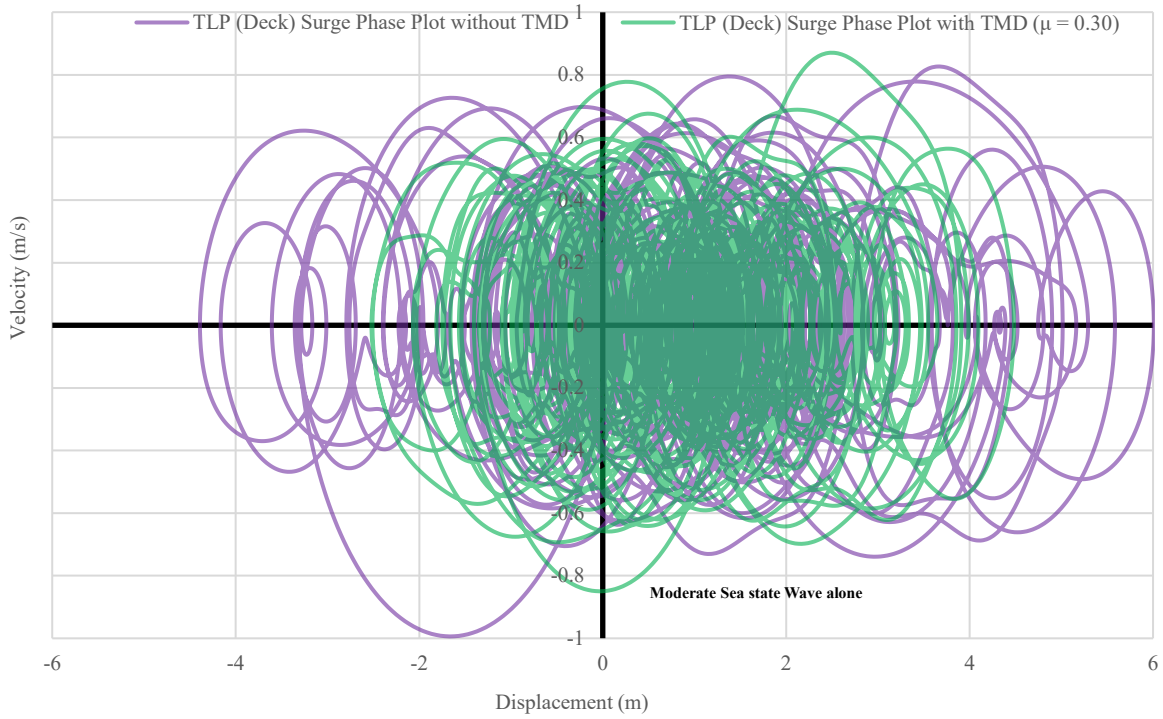

(a)

Figure 8 Wave alone case, (a) surge phase plot under moderate sea state, (b) surge phase plot under high sea state, (c) surge phase plot under very high sea state.

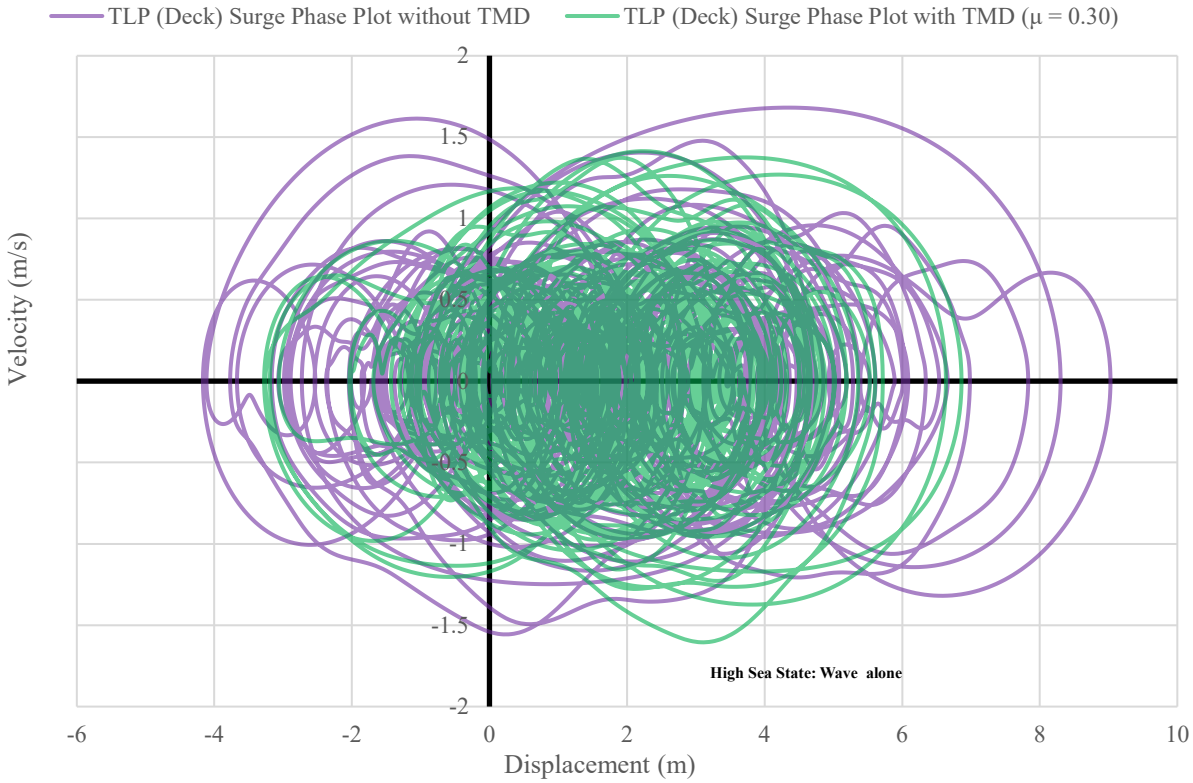

(b)

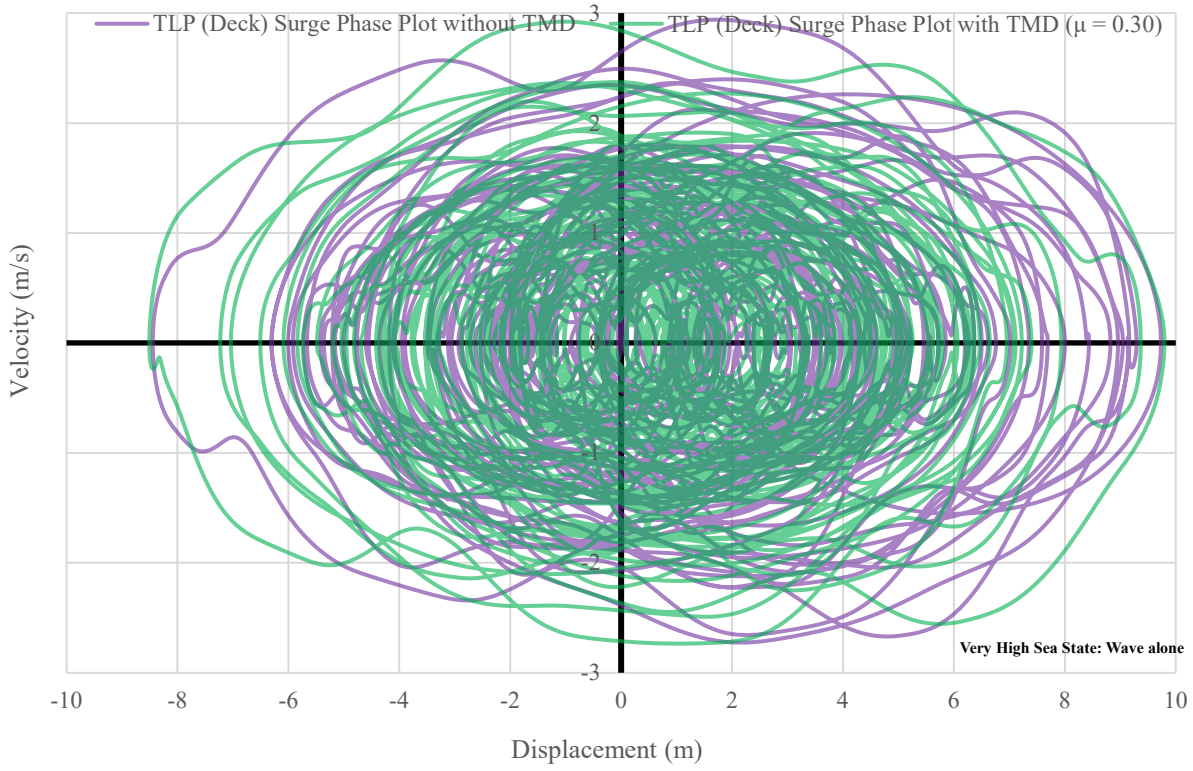

(c)

Figure 8 (continued) Wave alone case, (a) surge phase plot under moderate sea state, (b) surge phase plot under high sea state, (c) surge phase plot under very high sea state.

Table 5 TLP response statistics without TMD.

Statistics		Response without TMD								
		SS-1	SS-2	SS-3	SS-4	SS-5	SS-6	SS-7	SS-8	SS-9
Deck Surge Displacements (m)	Mean	0.901	1.231	0.872	0.901	1.235	0.920	1.152	1.587	1.089
	Standard Deviation	1.744	2.266	3.165	1.743	2.256	3.150	1.974	2.318	2.968
	RMS	1.700	2.233	2.843	1.700	2.227	2.842	1.980	2.433	2.738
	Minimum	-4.391	-5.038	-8.444	-4.389	-5.010	-8.146	-3.427	-4.164	-7.501
	Maximum	6.007	7.416	9.731	6.007	7.428	9.672	5.905	9.027	10.074
Deck Heave Displacements (m)	Mean	-0.059	-0.217	-0.764	-0.059	-0.218	-0.780	-0.060	-0.218	-0.769
	Standard Deviation	0.016	0.102	0.499	0.016	0.104	0.531	0.017	0.101	0.518
	RMS	0.053	0.208	0.790	0.053	0.209	0.817	0.054	0.208	0.803
	Minimum	-0.128	-0.779	-3.021	-0.128	-0.779	-3.022	-0.129	-0.775	-3.031
	Maximum	0.018	0.182	0.245	0.017	0.182	0.249	0.018	0.182	0.220
Deck Pitch Displacements (deg)	Mean	0.001	0.020	0.108	0.001	0.020	0.302	0.001	0.019	0.096
	Standard Deviation	0.035	0.122	0.573	0.035	0.119	0.633	0.035	0.115	0.583
	RMS	0.031	0.107	0.505	0.030	0.105	0.607	0.030	0.101	0.512
	Minimum	-0.188	-0.476	-2.356	-0.187	-0.476	-1.236	-0.187	-0.471	-1.690
	Maximum	0.194	0.742	3.082	0.194	0.742	3.081	0.194	0.745	3.022

Table 6 TLP response statistics with TMD.

Statistics		Response with TMD (μ = 0.30)								
		SS-1	SS-2	SS-3	SS-4	SS-5	SS-6	SS-7	SS-8	SS-9
Deck Surge Displacements (m)	Mean	0.886	1.223	0.869	0.887	1.226	0.878	1.145	1.614	1.074
	Standard Deviation	1.244	2.207	2.952	1.244	2.212	2.964	1.236	1.671	2.998
	RMS	1.323	2.185	2.665	1.323	2.190	2.677	1.459	2.012	2.758
	Minimum	-2.521	-5.365	-8.507	-2.520	-5.361	-8.373	-2.087	-3.275	-8.142
	Maximum	4.481	8.86946	9.795	4.482	8.873	10.035	4.552	6.860	9.914
Deck Heave Displacements (m)	Mean	-0.057	-0.217	-0.769	-0.057	-0.217	-0.786	-0.058	-0.215	-0.771
	Standard Deviation	0.015	0.102	0.486	0.015	0.102	0.537	0.016	0.101	0.524
	RMS	0.051	0.208	0.788	0.051	0.208	0.825	0.052	0.206	0.807
	Minimum	-0.128	-0.779	-3.020	-0.128	-0.779	-3.021	-0.128	-0.775	-3.029
	Maximum	0.017	0.183	0.247	0.017	0.183	0.247	0.018	0.182	0.222
Deck Pitch Displacements (deg)	Mean	0.001	0.020	0.045	0.001	0.021	0.048	0.001	0.018	0.114
	Standard Deviation	0.035	0.118	0.497	0.035	0.118	0.429	0.035	0.114	0.589
	RMS	0.030	0.104	0.432	0.030	0.104	0.374	0.030	0.100	0.520
	Minimum	-0.187	-0.477	-2.173	-0.187	-0.476	-1.739	-0.187	-0.472	-1.757
	Maximum	0.194	0.742	3.081	0.194	0.742	3.081	0.194	0.745	3.023

Table 7 Natural periods and damping ratios of TLP without TMD.

DoF	SS-1		SS-2		SS-3		SS-4		SS-5		SS-6		SS-7		SS-8		SS-9	
	Natural Periods (s)	Damping (%)	Natural Periods (s)	Damping (%)	Natural Periods (s)	Damping (%)	Natural Periods (s)	Damping (%)	Natural Periods (s)	Damping (%)	Natural Periods (s)	Damping (%)	Natural Periods (s)	Damping (%)	Natural Periods (s)	Damping (%)	Natural Periods (s)	Damping (%)
Surge	97.580	0.00244	97.39058	0.00677	97.4642	0.00186	97.55701	0.00358	97.39888	0.0042	97.44446	0.00433	97.55701	0.00358	97.39888	0.0042	97.44446	0.00433
Heave	2.01662	1.09E-05	2.01665	1.4668 E-5	2.0166	8.2196 E-6	2.01662	1.2069 E-5	2.01665	2.1353 E-5	2.0166	1.2445 E-5	2.01662	1.2069 E-5	2.01665	2.1353 E-5	2.0166	1.2445 E-5
Pitch	1.93062	0.00541	1.93058	0.00534	1.93062	0.00535	1.93062	0.00538	1.93058	0.00533	1.93062	0.00534	1.93062	0.00538	1.93058	0.00533	1.93062	0.00534

Table 8 Natural periods and damping ratios of TLP with TMD.

DoF	SS-1		SS-2		SS-3		SS-4		SS-5		SS-6		SS-7		SS-8		SS-9	
	Natural Periods (s)	Damping (%)	Natural Periods (s)	Damping (%)	Natural Periods (s)	Damping (%)	Natural Periods (s)	Damping (%)	Natural Periods (s)	Damping (%)	Natural Periods (s)	Damping (%)	Natural Periods (s)	Damping (%)	Natural Periods (s)	Damping (%)	Natural Periods (s)	Damping (%)
Surge	90.49998	7.26246	90.36587	7.24718	90.43443	7.23788	90.50056	7.26043	90.36481	7.2468	90.43826	7.23536	90.50056	7.26043	90.36595	7.24613	90.43826	7.23536
Heave	2.01661	1.3872 E-5	2.01665	2.0252 E-5	2.0166	1.1550 E-5	2.01661	7.9464 E-6	2.01665	2.5080 E-5	2.0166	9.3624 E-6	2.01661	7.9464 E-6	2.01665	2.2508 E-5	2.0166	9.3624 E-6
Pitch	1.93062	0.00761	1.93058	0.00762	1.93062	0.00761	1.93061	0.00762	1.93058	0.00758	1.93062	0.00762	1.93061	0.00762	1.93058	0.00759	1.93062	0.00762

4.3 Combined wave, wind, and current

The surge responses for the ISSC TLP without and with TMD having a mass ratio of $\mu = 0.3$ under combined wind, wave, and current conditions of various sea state environments are shown in **Figures 9a - 9c**. The surge response time history shows a substantial reduction in the surge motion for moderate as well as high sea states in the presence of the TMD. The surge response of the TMD is highlighted with an orange dotted line in **Figure 9**. It has been observed that the reduction in maximum surge responses is about 23 percent for moderate sea states, about 24 percent for high sea states, and about 2 percent for very high sea states. The rms values for the surge responses show a reduction of about 26 percent for moderate; and about 17 percent for high sea states; but no reduction for very high sea states. The influence of the TMD on heave and pitch responses is absent. Here also, the mean, rms, and maximum responses in the heave and pitch are almost unchanged.

Figures 10a - 10c show the power spectral densities in the surge, heave, and pitch, respectively. The PSD plots show a significant reduction in the energy content in the surge degree of freedom, about 65 percent for moderate, and close to 60 percent for the high-sea state. However, it has been observed that the TMD is ineffective when the sea state is very high. The other degrees of freedom, heave and pitch, do not show much variation in PSD plots. The shifts in the natural

frequencies with and without TMD are shown with dotted lines in the PSD plots. It is seen that shifts in the natural frequencies due to the presence of the TMD are marginal. The peak in the surge PSD occurs close to the surge natural frequency for both models, which needs to be taken into consideration for the detailed design by altering the tendon stiffness. **Figures 11a - 11c** show the phase plots for the surge motion under different sea state environments with combined wave, wind, and current conditions. The phase plots show the good recentering ability of the platform with and without TMD, which is desirable. This shows that the recentering capabilities of the platform are not affected by the additional damping induced in the system due to the presence of the TMD. The period and damping in active degrees of freedom (i.e., surge, heave, and pitch) for the different sea state conditions, obtained from the stability analysis, are presented in **Tables 7** and **8**. As can be seen from the tables, there is a reduction of about 7 percent in the period of ISSC TLP with TMD in surge motion, as compared to that of ISSC TLP without TMD for all the load cases. The surge natural frequencies in the presence of the TMD are still outside the frequency bandwidth of waves. In addition, the system damping is substantially increased in surge degree of freedom with the use of TMD. It is to be noted that the other degrees of freedom, heave and pitch, have remained almost unchanged for all the load cases. This indicates that the TMD is effective in dampening the surge motion of the system against external loads.

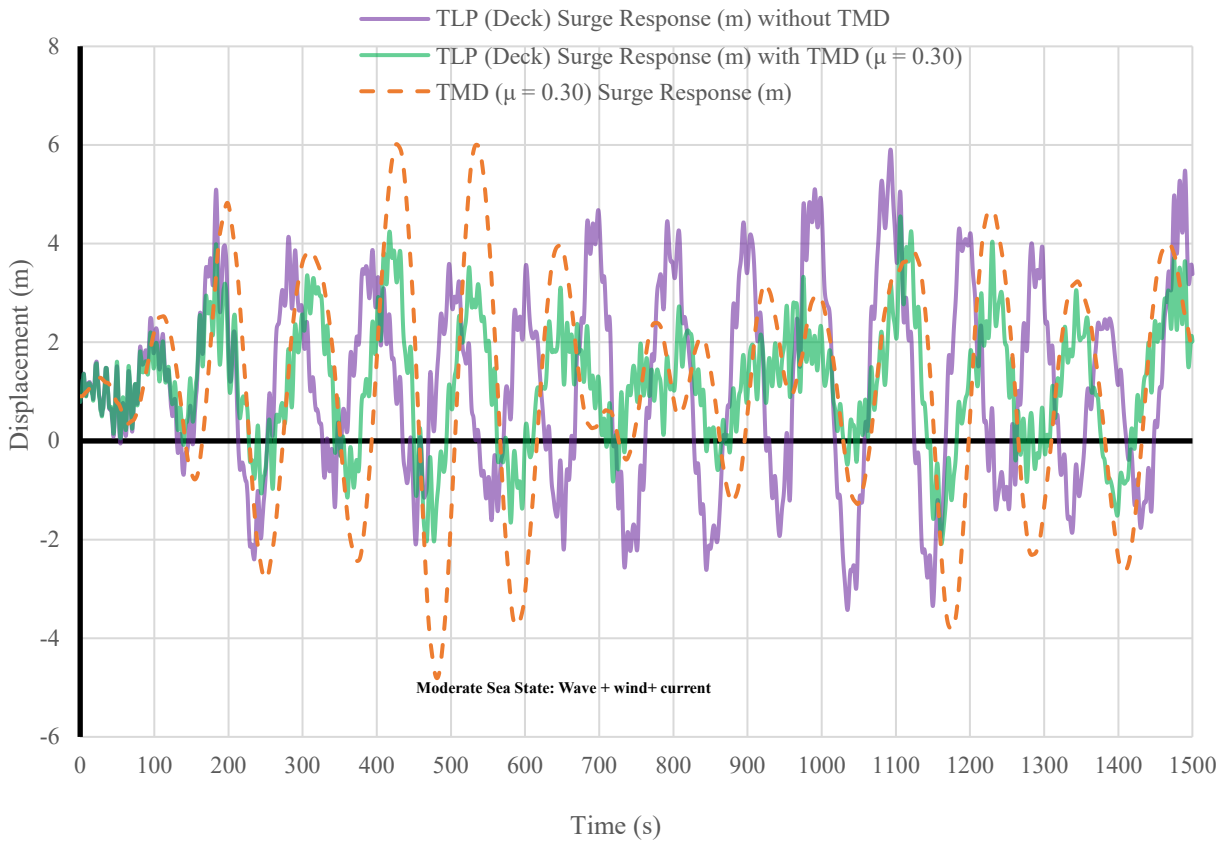

(a)

Figure 9 Wave + Wind + Current case, (a) surge responses under moderate sea state, (b) surge responses under high sea state, (c) surge responses under very high sea state.

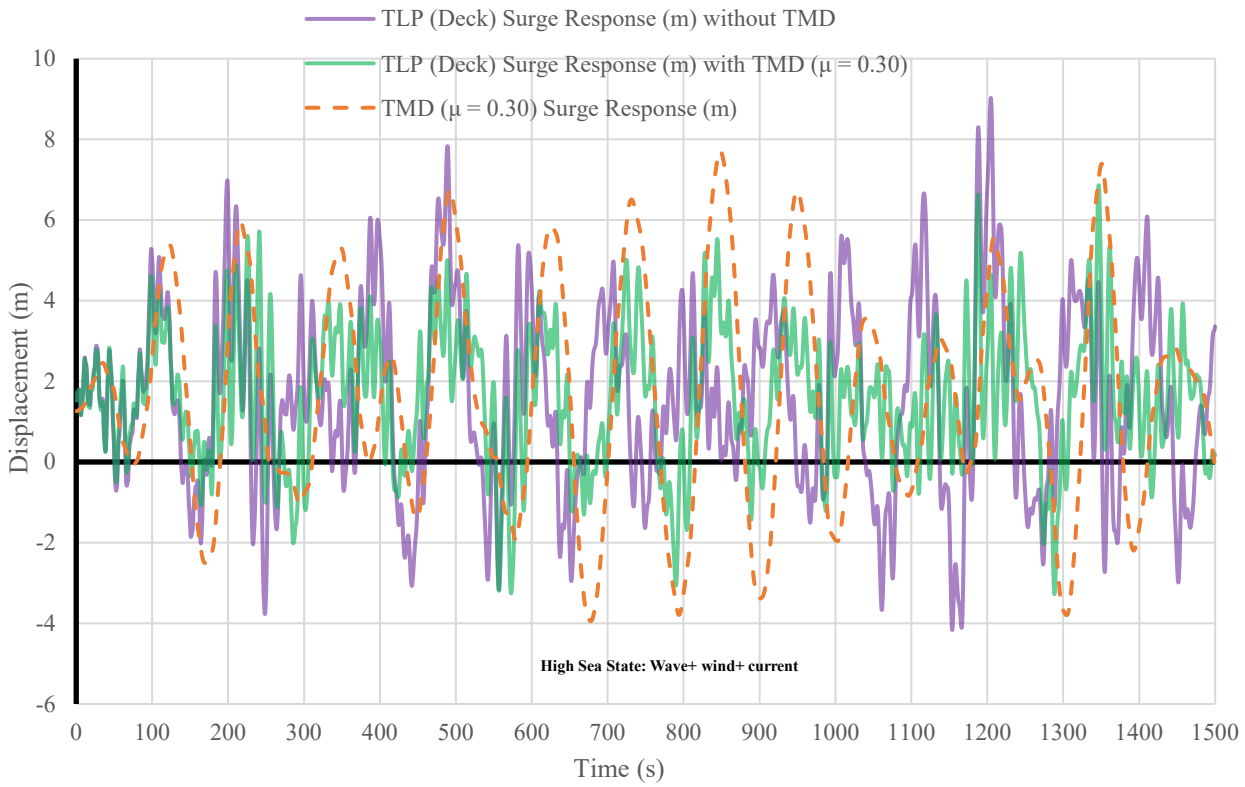

(b)

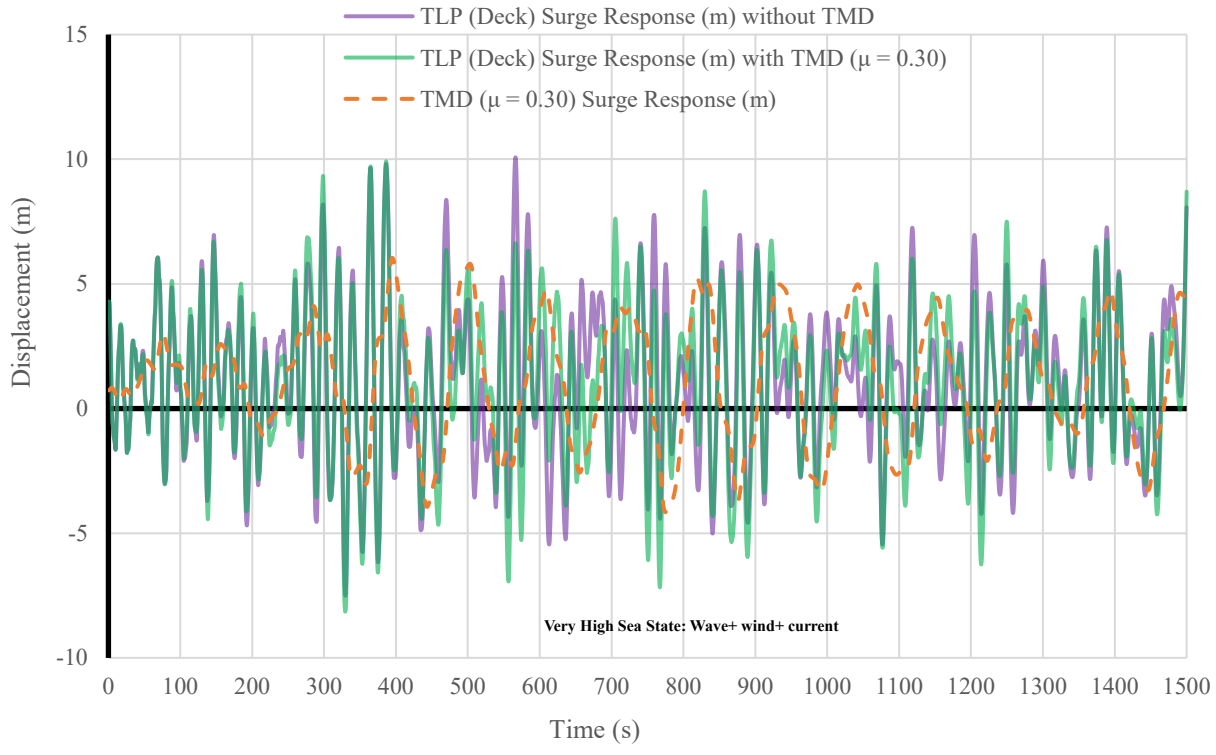

(c)

Figure 9 (continued) Wave + Wind + Current case, (a) surge responses under moderate sea state, (b) surge responses under high sea state, (c) surge responses under very high sea state.

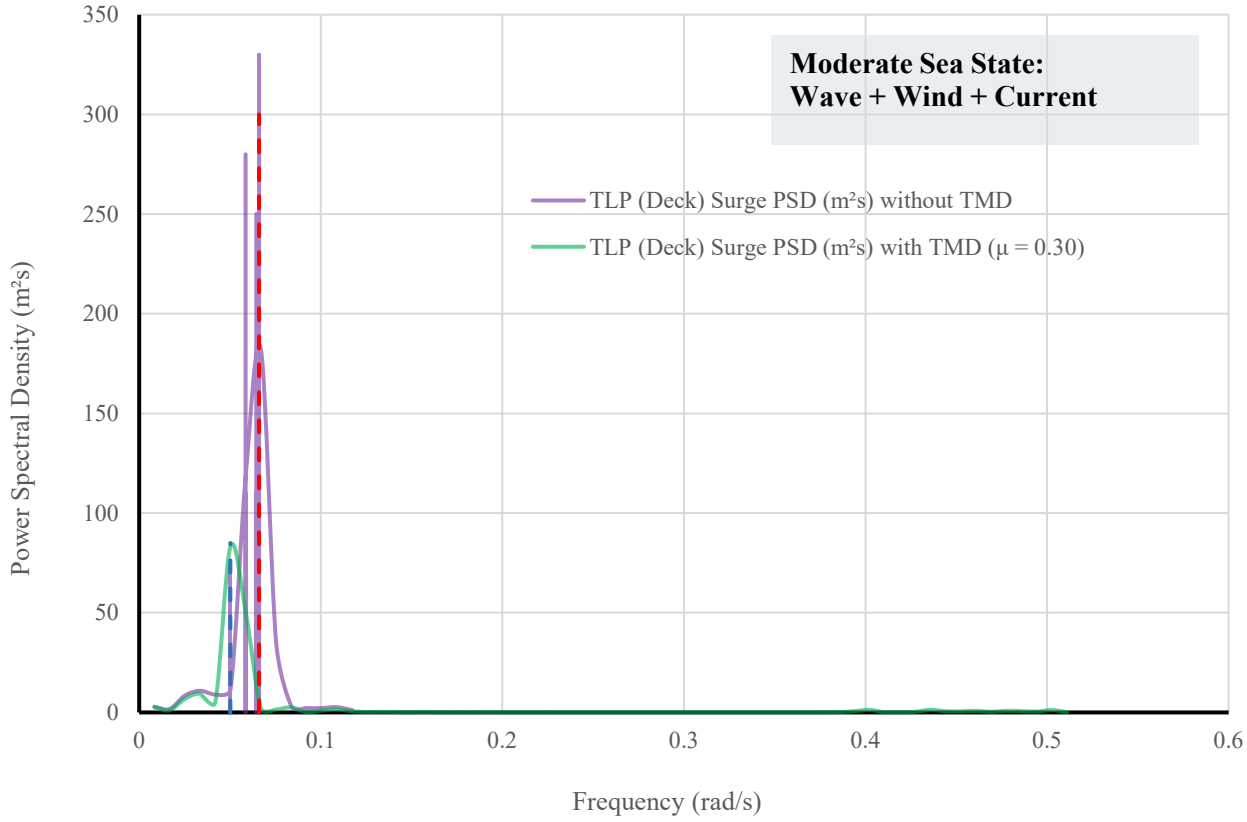

(a)

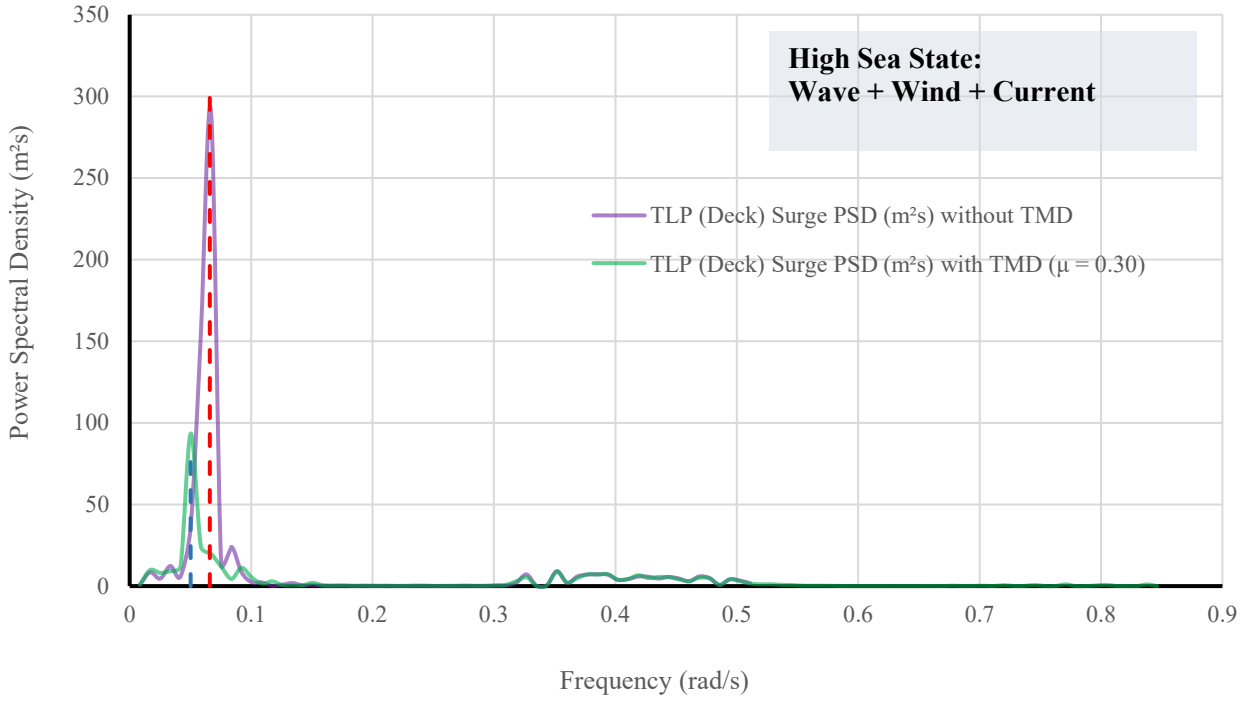

(b)

Figure 10 Wave + Wind + Current case, (a) surge PSD under moderate sea state, (b) surge PSD under high sea state, (c) surge PSD under very high sea state.

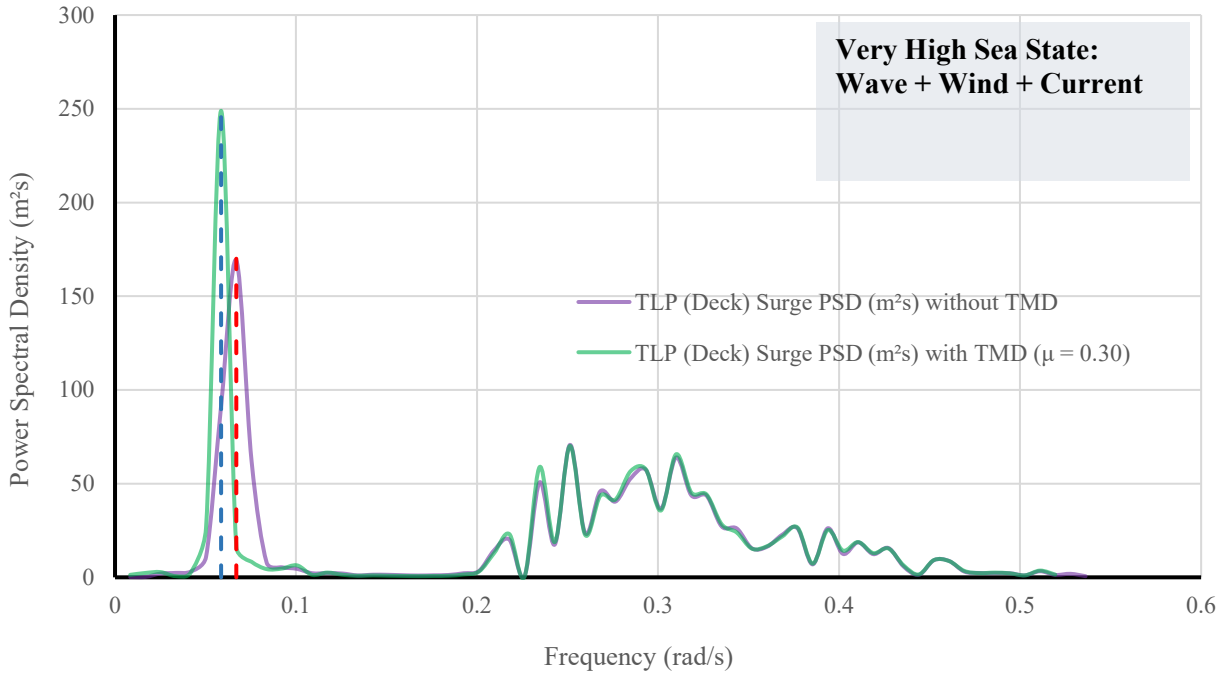

(c)

Figure 10 (continued) Wave + Wind + Current case, (a) surge PSD under moderate sea state, (b) surge PSD under high sea state, (c) surge PSD under very high sea state.

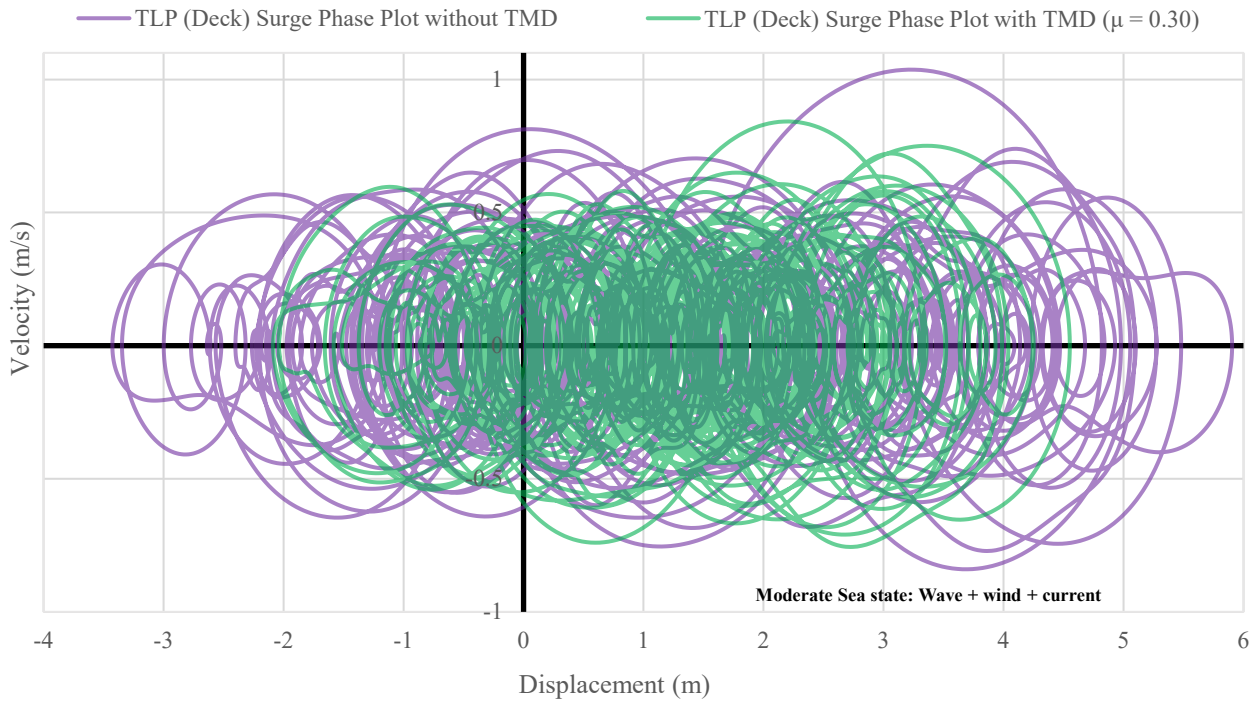

(a)

Figure 11 Wave + Wind + Current case, (a) surge phase plot under moderate sea state, (b) surge phase plot under high sea state, (c) surge phase plot under very high sea state.

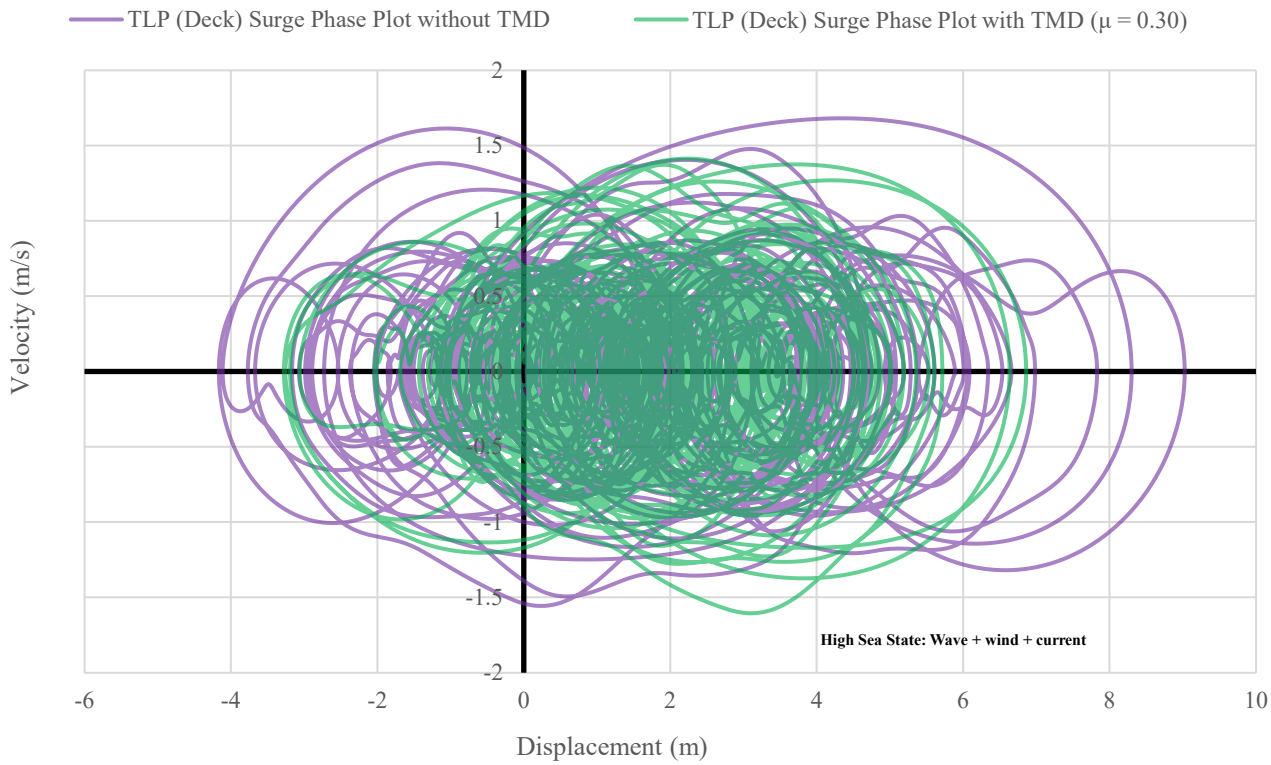

(b)

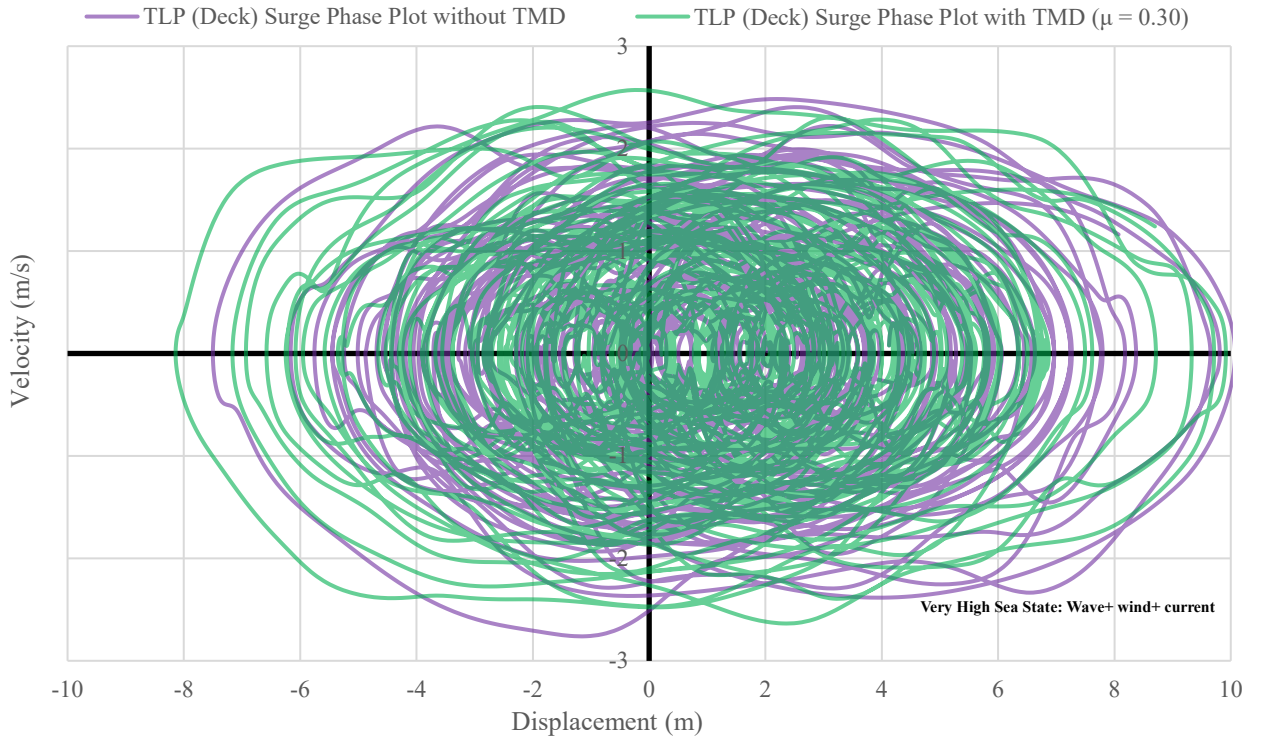

(c)

Figure 11 (continued) Wave + Wind + Current case, (a) surge phase plot under moderate sea state, (b) surge phase plot under high sea state, (c) surge phase plot under very high sea state.

5. Conclusions

This study evaluates the performance of TLP under the presence of TMD. The surge response, being a compliant platform, is examined in detail for the ISSC TLP under three distinct combinations of load, namely wave, wind, and current, for a mass ratio of 0.3. The results show that the novel TMD helps reduce the response under moderate sea states in particular; the reduction is about 26 %, but it is minimal under high and very high sea states. The heave and pitch responses showed no significant reduction in the presence of TMD, but there is a reduction of the energy content of the response under all sea states, as seen from the PSD plots. Although there is an increase in the surge damping, the platform oscillates with respect to its mean position, maintaining the recentering capabilities. The shift in the frequency of the first peak, as seen in the surge PSD plots, caused a marginal shift in the displacement origin, but still exhibited a steady response cycle. This is confirmed from the phase plots.

References

Abou-Rayan, A. M., & El-Gamal, A. R. (2013). Wave-induced motion of a triangular tension leg platforms in deep waters. *Ocean Systems Engineering, 3*(2), 149-165. https://doi.org/10.12989/ose.2013.3.2.149

Ayorinde, E. O., & Warburton, G. B. (1980). I am minimizing structural vibrations with absorbers. *Earthquake Engineering & Structural Dynamics, 8*(3), 219-236. https://doi.org/10.1002/eqe.4290080303

Chandrasekaran, S., & Jamshed, N. (2017). *Springing and ringing response of offshore triceratops* (pp. 1-6). In Proceedings of the 34th International Conference on Ocean, Offshore and Arctic Engineering. Newfoundland, Canada. https://doi.org/10.1115/OMAE2015-41551

Chandrasekaran, S. (2015). *Dynamic analysis and design of offshore structures*. Springer New Delhi. https://doi.org/10.1007/978-81-322-2277-4

Chandrasekaran, S., Chandak, N. R., & Anupam, G. (2006a). Stability analysis of TLP tethers. *Ocean Engineering, 33*(3-4), 471-482. https://doi.org/10.1016/j.oceaneng.2005.04.015

Chandrasekaran, S., & Gaurav. (2008). Offshore triangular tension leg platform earthquake motion analysis under distinctly high sea waves. *Ships and Offshore Structures, 3*(3), 173-184. https://doi.org/10.1080/17445300802051681

Chandrasekaran, S., & Jain, A. (2016). *Ocean structures*. CRC Press. https://doi.org/10.1201/9781315366692-7

Chandrasekaran, S., & Jain, A. K. (2002). Triangular configuration tension leg platform behavior under random sea wave loads. *Ocean Engineering, 29*(15), 1895-1928. https://doi.org/10.1016/S0029-8018(01)00111-1

Chandrasekaran, S., & Jain, A. K. (2001). Dynamic behavior of square and triangular offshore tension leg platforms under regular wave loads. *Ocean Engineering, 29*(3), 279-313. https://doi.org/10.1016/S0029-8018(00)00076-7

Chandrasekaran, S., Jain, A. K., & Chandak, N. R. (2007a). Response behavior of triangular tension leg platforms under regular waves using stokes nonlinear wave theory. *Journal of Waterway, Port, Coastal, and Ocean Engineering, 133*(3), 230-237. https://doi.org/10.1061/(asce)0733-950x(2007)133:3(230)

Chandrasekaran, S., Jain, A. K., & Chandak, N. R. (2006b). Seismic analysis of offshore triangular tension leg platforms. *International Journal of Structural Stability and Dynamics, 6*(1), 97-120. https://doi.org/10.1142/S0219455406001848

Chandrasekaran, S., Jain, A. K., & Chandak, N. R. (2004). Influence of hydrodynamic coefficients in the response behavior of triangular TLPs in regular waves. *Ocean Engineering, 31*(17-18), 2319-2342. https://doi.org/10.1016/j.oceaneng.2004.06.005

Chandrasekaran, S., Jain, A. K., & Gupta, A. (2007b). Influence of wave approach angle on TLP's response. *Ocean Engineering, 34*(8-9), 1322-1327. https://doi.org/10.1016/j.oceaneng.2006.08.007

Chandrasekaran, S., Jain, A. K., Gupta, A., & Srivastava, A. (2007c). Response behaviour of triangular tension leg platforms under impact loading. *Ocean Engineering,* 34, 45-53. https://doi.org/10.1016/j.oceaneng.2006.01.002

Chandrasekaran, S., & Koshti, Y. (2013). Dynamic analysis of a Tension Leg Platform under extreme waves. *Journal of Naval Architecture and Marine Engineering, 10*(1), 59-68. https://doi.org/10.3329/jname.v10i1.14518

Chandrasekaran, S., Kumar, D., & Ramanathan, R. (2013). Dynamic response of tension leg platform with tuned mass dampers. *Journal of Naval Architecture and Marine Engineering, 10*(2), 149-157. http://dx.doi.org/10.3329/jname.v10i2.16184

Chandrasekaran, S., Kumar, D., & Ramanthan, R. (2015). Response control of tension leg platform with passive damper: experimental investigations. *Ships and Offshore Structures, 12*(2), 171-181. https://doi.org/10.1080/17445302.2015.1119666

Chandrasekaran, S., & Nagavinothini, R. (2020). *Offshore compliant platforms.* John Wiley & Sons. https://doi.org/10.1002/9781119669791

Chandrasekaran, S., & Nassery, J. (2017). Ringing response of offshore triceratops. *Innovative Infrastructure Solutions, 2*, 23. https://doi.org/10.1007/s41062-017-0092-5

Chandrasekaran, S., Sharma, A., & Srivastava, S. (2007d). Offshore triangular TLP behaviour using dynamic Morison equation. *Journal of Structural Engineering, 34*(4), 291-296.

Chandrasekaran, S., & Suja, T. P. (2023). *Response control of tension leg platform under random waves using tuned mass damper*. In Proceedings of the 33rd International Ocean and Polar Engineering Conference. Ottawa, Canada.

Chatterjee, T., & Chakraborty, S. (2014). Vibration mitigation of structures subjected to random wave forces by liquid column dampers. *Ocean Engineering, 87*, 151-161. https://doi.org/10.1016/j.oceaneng.2014.05.004

Chou, F. S. F., Ghosh, S., & Kypke, D. A. (1980). *Analytical approach to the design of a tension leg platform*. In Proceedings of the Offshore Technology Conference. Houston, Texas. https://doi.org/10.4043/3883-ms

Eatock Taylor, R., & Jefferys, E. R. (1986). Variability of hydrodynamic load predictions for a tension leg platform. *Ocean Engineering, 13*(5), 449-490. https://doi.org/10.1016/0029-8018(86)90033-8

Hongbo, W., Xiaolin, M., & Chaohe, C. (2022). Cross-correlation analysis of wind speeds and displacements of a long-spanbridge with GNSS under extreme wind conditions. *Maritime Technology and Research, 4*(3), 254407. https://doi.org/10.33175/mtr.2022.254407

Kandasamy, R., Cui, F., Townsend, N., Foo, C. C., Guo, J., Shenoi, A., & Xiong, Y. (2016). A review of vibration control methods for marine offshore structures. *Ocean Engineering, 127*, 279-297. https://doi.org/10.1016/j.oceaneng.2016.10.001

Nagavinothini, R., & Chandrasekaran, S. (2019). Dynamic analyses of offshore triceratops in ultra-deep waters under wind, wave, and current. *Structures, 20*, 279-289. https://doi.org/10.1016/j.istruc.2019.04.009

Sreenivasan, H., Krishna, S., Rao, M. H. V. R., & Vij, R. K. (2021). Postulated failure analyses of tension leg platform (top) restraining system under the influence of varying sea-state conditions. *Structural Integrity and Life, 21*(S), S29-S37.

Srinivasan, C., Gaurav, G., Serino, G., & Miranda, S. (2011). Ringing and springing response of triangular TLPs. *International Shipbuilding Progress, 58*(2-3), 141-163. https://doi.org/10.3233/ISP-2011-0073

Srinivasan, C., & Purushotham, C. (2024). Dynamic analysis of offshore triceratops supporting wind turbine: Preliminary studies. *Maritime Technology and Research, 6*(1), 265564. doi.org/10.33175/mtr.2024.265564

Tabeshpour, M. R., & Malayjerdi, E. (2021). Surge motion passive control of TLP with double horizontal tuned mass dampers. *International Journal of Acoustics and Vibration, 26*(1), 4-8. https://doi.org/10.20855/ijav.2020.25.11273

Taflanidis, A. A., Angelides, D. C., & Scruggs, J. T. (2009). Simulation-based robust design of mass dampers for response mitigation of tension leg platforms. *Engineering Structures, 31*(4), 847-857. https://doi.org/10.1016/j.engstruct.2008.11.014

Wang, Z. M., & Kim, C. H. (2001). *Nonlinear response of ISSC TLP in high and steep random waves*. In Proceedings of the 11th International Offshore and Polar Engineering Conference, Stavanger, Norway.

Xu, Wei, N., & Yao, W. (2022). The stability analysis of tension-leg platforms under marine environmental loads via altering the connection angle of tension legs. *Water, 14*(3), 283. https://doi.org/10.3390/w14030283

Yoneya, T., & Yoshida, K. (1981). Dynamics of tension leg platforms in waves. *Journal of Energy Resources Technology, 104*(1), 20-28. https://doi.org/10.1115/1.3230375